



HAL
open science

Oversampled phase tracking in digital communications with large excess bandwidth

Jordi Vilà Valls, Jean-Marc Brossier, Laurent Ros

► **To cite this version:**

Jordi Vilà Valls, Jean-Marc Brossier, Laurent Ros. Oversampled phase tracking in digital communications with large excess bandwidth. *Signal Processing*, 2010, 90 (3), pp.821-833. 10.1016/j.sigpro.2009.08.012 . hal-00447410

HAL Id: hal-00447410

<https://hal.science/hal-00447410>

Submitted on 14 Jan 2010

HAL is a multi-disciplinary open access archive for the deposit and dissemination of scientific research documents, whether they are published or not. The documents may come from teaching and research institutions in France or abroad, or from public or private research centers.

L'archive ouverte pluridisciplinaire **HAL**, est destinée au dépôt et à la diffusion de documents scientifiques de niveau recherche, publiés ou non, émanant des établissements d'enseignement et de recherche français ou étrangers, des laboratoires publics ou privés.

Oversampled phase tracking in digital communications with large excess bandwidth[☆]

Jordi Vilà-Valls, Jean-Marc Brossier, Laurent Ros

GIPSA-Lab, Department Image Signal, BP 46 - 38402 Saint Martin d'Hères - FRANCE

Abstract

This paper deals with the on-line carrier phase estimation in a digital receiver. We consider a Brownian phase evolution in a Data Aided scenario. The proposed study uses an oversampled signal model after matched filtering, leading to a coloured reception noise and a non-stationary power signal. The contribution of this paper is twofold. First, we derive the Bayesian Cramér-Rao Bound for this estimation problem. Then, based on a state-space model formulation of the problem, we propose an Extended Kalman Filter to approach this lower bound for a BOC shaping pulse. Our numerical results illustrate the gain resulting from the use of an oversampled version of the received signal to estimate the phase offset, obtaining better performances than using a classical synchronizer.

Key words: Phase estimation, BCRB, Extended Kalman Filter, oversampling, carrier synchronization, GALILEO, BOC

1. Introduction

Synchronization is a fundamental part in modern digital receivers. A synchronizer has to estimate parameters such as carrier frequency, carrier phase and timing epoch. This knowledge is required to recover the signal of interest correctly. In this paper, we focus our attention on the phase estimation problem. Many methods for estimating the phase introduced by

[☆]Part of this work was presented in conferences [12] and [13].

Email addresses: `jordi.vilavalls@gipsa-lab.inpg.fr` (Jordi Vilà-Valls),
`jean-marc.brossier@gipsa-lab.inpg.fr` (Jean-Marc Brossier),
`laurent.ros@gipsa-lab.inpg.fr` (Laurent Ros)

an unknown channel have been proposed over the past decades, from Phase Locked Loops (PLL) to the most sophisticated signal processing techniques. Among lower bounds on the estimation performance than can be used as a benchmark, the family of Cramér-Rao Bounds (CRBs) has been shown to give accurate results in many scenarios [1]. Several Cramér-Rao lower bounds are given in the literature.

For constant phase-offset estimation in the so-called Data-Aided (DA) scenario, Rife *et al.* [20] derive CRB closed-form expressions; Cowley [21] does so in the Non-Data-Aided (NDA) scenario. Since these bounds are frequently analytically untractable, the looser *modified* CRB (MCRB) [18, 19] is widely used to reduce the complexity.

For time-varying parameter estimation, an analytical expression of a general *on-line* recursive Bayesian CRB (BCRB) is given by Tichavský [17]. Bay *et al.* [15] introduce an Asymptotic BCRB (ABCRB) and provide an analytical expression of the *off-line* CRB and BCRB.

Several algorithms attempt to approach optimal performance given by lower bounds. The Kalman Filter (KF) [5],[6], presented in early 1960s is optimal for parameter estimation in linear Gaussian problems [7, 8].

When dealing with nonlinear filtering problems, the Extended Kalman Filter (EKF) approximates the problem to apply the KF solution. The EKF has been proved to be a powerful low-complexity solution for slightly nonlinear problems. Some contributions show the use of EKF for carrier phase recovery and frequency tracking [22, 23, 24, 25]. Other solutions to cope with nonlinear filtering problems include the well-known Particle Filter (PF). Although this technique has been largely applied during the last ten years [9], its performance gain is usually not worth its high implementation complexity for slightly nonlinear problems with slowly varying parameters like phase estimation [14].

Most of the lower bounds assume a white observation noise and a stationary signal.

In [12], we calculate a lower bound for an *oversampled* (regarding the symbol time interval) signal model after matched filtering, this implies dealing with a *coloured reception noise* and taking into account the non-stationarity of the digital signal power (cyclostationarity when transmitting a random sequence). Although this scenario is standard in satellite radio-localization based on a Binary Offset Carrier (BOC) time-limited shaping pulse modulation, there is no theoretical study concerning the performance of oversampled phase offset estimation in this context (to the best of our knowledge).

In this contribution, we first derive a closed-form expression of the on-line Bayesian Cramér-Rao Bound (BCRB) for phase estimation in the Data Aided (DA) scenario, assuming a Brownian phase evolution. The BCRB we present here is simpler than the one we have presented in [12].

Secondly, we investigate the use of an EKF based algorithm to approach this bound. We have thus to jointly estimate the coloured noise and the phase offset. The study allows to measure the potential gain for phase estimation provided by the use of the fractionally-spaced processing after matched filtering, instead of the symbol time-spaced signal.

This paper is organized as follows. Section II sets the signal model. Section III recalls the BCRB expressions and derives the BCRB for this estimation problem. Section IV presents the EKF and derives the expressions of the filter in the oversampled phase estimation scenario. Finally, in Section V, the numerical results for the EKF for a BPSK transmission are presented and interpreted together with the BCRB. **We also compare the EKF performance with a Particle Filter algorithm and we do the analysis of real world conditions.** The conclusion is given in Section VI.

Notations: italic indicates a scalar quantity, as in a ; boldface indicates a vector quantity, as in \mathbf{a} and capital boldface indicates a matrix quantity as in \mathbf{A} . The $(k, l)^{th}$ entry of a matrix \mathbf{A} is denoted $[\mathbf{A}]_{k,l}$. The matrix transpose and self-adjoint operators are denoted by the superscripts T and H respectively as in \mathbf{A}^T and \mathbf{A}^H . $\Re(\cdot)$, $\Im(\cdot)$ and $(\cdot)^*$ are the real part, the imaginary part and conjugate of a complex number or matrix, respectively. E_x denotes the expectation over x . $\nabla_{\boldsymbol{\theta}}$ and $\Delta_{\boldsymbol{\psi}}^{\boldsymbol{\theta}}$ represent the first and second-order partial derivatives operator *i.e.*, $\nabla_{\boldsymbol{\theta}} = \left[\frac{\partial}{\partial \theta_1} \cdots \frac{\partial}{\partial \theta_K} \right]^T$ and $\Delta_{\boldsymbol{\psi}}^{\boldsymbol{\theta}} = \nabla_{\boldsymbol{\psi}} \nabla_{\boldsymbol{\theta}}^T$. $\mathbf{1}$ stands for the all-ones matrix.

2. Signal Model

We propose a signal model for the transmission of a known complex-valued sequence $\{a_m\}_{m \in \mathbb{Z}}$ over an Additive White Gaussian Noise (AWGN) channel affected by a carrier phase offset $\theta(t)$.

2.1. Oversampled Signal Model

2.1.1. Discrete-time general formulation

The received complex baseband signal after matched filtering is

$$y(t) = \left[\left\{ T \sum_m a_m \Pi(t - mT) \right\} e^{i\theta(t)} + n(t) \right] * \Pi^*(-t)$$

where $T, \Pi(t)$ and $n(t)$ stands for the symbol period, shaping pulse and circular Gaussian noise with a known bilateral power spectral density (psd) N_0 .

We define the filtered coloured noise

$$b(t) = [n(t)] * \Pi^*(-t)$$

and the shaping function $\tilde{g}_m(t)$ as

$$\tilde{g}_m(t) = T \int_{-\infty}^{+\infty} \Pi^*(-\alpha) e^{i\theta(t-\alpha+mT)} \Pi(t-\alpha) d\alpha$$

Then the received signal can be written as

$$y(t) = \sum_m a_m \tilde{g}_m(t - mT) + b(t)$$

Hereafter, we suppose a shaping pulse Π with support in $[0, T)$ and a slow varying phase during a period T . **This last assumption is usual in satellite communications because the phase variation (due to oscillators phase noise, Doppler effects, ...) in one symbol period is weak.** Phase noise introduced by oscillators is usually lower than phase variation due to Doppler shifts [3]. Concerning the Doppler effects, it is easy to verify the assumption in a real world scenario such as Galileo systems: in the worst cases, the maximum Doppler shift is about 20 kHz. If we assume a chip rate $\frac{1}{T} = 1$ Mchip/sec, the maximal phase variation in one period is about $\Delta_\theta = 0.1$ rad, corresponding to a weak jitter amplitude ($0.1/2\pi = 1.6\%$) or to a variation of 0.01 rad^2 . In this paper we consider a maximal phase noise variance $\sigma_w^2 = 0.1 \text{ rad}^2$, to take into account possible stronger phase noise effects while still verifying the assumption of weak variation into one period T .

In this case we can approximate $\tilde{g}_m(t)$ by

$$\tilde{g}_m(t) \approx g(t) e^{i\theta(t+(m+\frac{1}{2})T)} \quad (1)$$

where

$$g(t) = T \int_{-T}^0 \Pi^*(-\alpha) \Pi(t-\alpha) d\alpha$$

If the received signal is fractionally-spaced at $t_k = k\frac{T}{S} + \tau$, where S is an integer oversampling factor and τ a known offset from the optimum sampling instants (we suppose $0 \leq \tau < \frac{T}{S}$), we have that

$$y\left(k\frac{T}{S} + \tau\right) = \sum_m a_m \tilde{g}_m\left(k\frac{T}{S} + \tau - mT\right) + b\left(k\frac{T}{S} + \tau\right)$$

and from (eq. 1) we have that

$$y\left(k\frac{T}{S} + \tau\right) = e^{i\theta(k\frac{T}{S} + \tau + \frac{T}{2})} A_k + b\left(k\frac{T}{S} + \tau\right)$$

where

$$A_k = \sum_m a_m g\left(k\frac{T}{S} + \tau - mT\right). \quad (2)$$

We can finally write the received oversampled signal as

$$y_k = A_k e^{i\theta_k} + b'_k$$

where k refers to t_k instants. Note that the noise b'_k is coloured with variance σ_n^2 , where $\sigma_n^2 = N_0 \times \frac{g(0)}{T}$ is the variance of the AWGN $n(t)$ measured in the noise equivalent bandwidth of the receiver filter $\Pi^*(-t)$.

We can define the symbol index $p = \lfloor \frac{k}{S} \rfloor$, or equivalently, $k = pS + s$ with s ($s = 0, \dots, S - 1$) the sub-symbol index (*i.e.* the position inside the symbol interval). $\{A_k\}_{k \in \mathbb{Z}}$ is a non-stationary power sequence for $S > 1$, even if $\{a_m\}_{m \in \mathbb{Z}}$ is a stationary power symbol sequence ($a_m^2 = 1$).

In fig.1, we show, as an example, the transmission of a symbol sequence \mathbf{a} of length 7 symbols, using the BOC shaping pulse (see fig.2), over a perfect channel (without phase shift, without noise, and for $\tau = 0$), and the corresponding received signal after match filtering. From this figure, we can see, marked with circles, the samples corresponding to $S = 1$ (symbol reference points). Marked with big squares (symbol mid-points) we have the samples that we add when using $S = 2$ instead of $S = 1$. And finally, marked with little squares we have the samples obtained when using an oversampling $S = 4$.

In this case, we can see that some of the intermediate samples are null, so these samples do not contribute to the measurement, and so they do not give us information to improve the estimation.

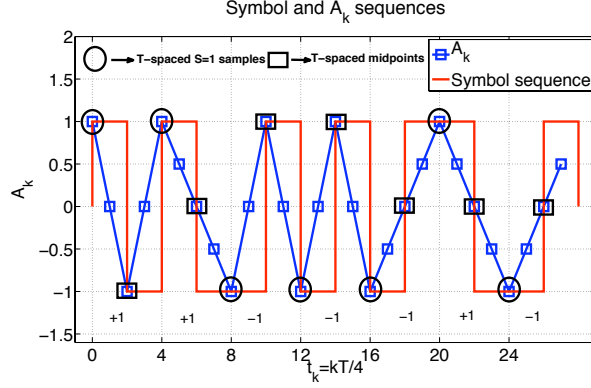


Figure 1: Symbol sequence and received signal over a perfect channel. Set of samples for $S = 1, 2$ and 4.

2.1.2. Discrete-time re-formulation for the noise

The $\frac{T}{S}$ -spaced sequence of noise $\{b'_k\}_{k \in \mathbb{Z}}$ is defined in the previous section from an analog noise $n(t)$. Our motivation now is to replace this time series by another sequence $\{b_k\}_{k \in \mathbb{Z}}$ with the same statistical properties, but obtained using a discrete-time formulation. This will be useful for the final state-space model formulation. We can write that

$$\begin{aligned} b'_k &= \int_0^T n\left(\alpha + k\frac{T}{S} + \tau\right) \Pi^*(\alpha) d\alpha \\ &= \sum_{j=0}^{S-1} \int_{j\frac{T}{S}}^{(j+1)\frac{T}{S}} n\left(\alpha + k\frac{T}{S} + \tau\right) \Pi^*(\alpha) d\alpha \end{aligned}$$

For N measurements, the $N \times N$ covariance matrix $\mathbf{\Gamma}$ of the observation noise depends on the oversampling factor S . **As an example, for $S = 2$, we have a tridiagonal matrix**

$$\mathbf{\Gamma} = \frac{N_0}{T} \begin{pmatrix} g(0) & g(-\frac{T}{2}) & & & \\ g(\frac{T}{2}) & \ddots & \ddots & & \\ & \ddots & \ddots & g(-\frac{T}{2}) & \\ & & & g(\frac{T}{2}) & g(0) \end{pmatrix} \quad (3)$$

The random variables

$$Z_{k,j} = \int_{j\frac{T}{S}}^{(j+1)\frac{T}{S}} n\left(\alpha + k\frac{T}{S} + \tau\right) \Pi^*(\alpha) d\alpha$$

are zero-mean Gaussian. For a fixed k , $Z_{k,j}$ are independent in j . Their variance is equal to

$$\mathbb{E} (|Z_{k,j}|^2) = N_0 \int_{j\frac{T}{S}}^{(j+1)\frac{T}{S}} |\Pi(\alpha)|^2 d\alpha$$

We define a zero-mean, unit variance, stationary Gaussian i.i.d sequence $\{n_k\}_{k \in \mathbb{Z}}$ and

$$\Pi_j = \left\{ N_0 \int_{j\frac{T}{S}}^{(j+1)\frac{T}{S}} |\Pi(\alpha)|^2 d\alpha \right\}^{\frac{1}{2}}$$

Hence, the noise samples b'_k have the same statistical properties than samples b_k , and are obtained by a $\frac{T}{S}$ -spaced filtering of the time serie n_k :

$$b_k = \sum_{j=0}^{S-1} \Pi_j n_{k-j-1}$$

2.2. Phase-offset Evolution Model

In practice, we have to consider jitters introduced by **oscillators imperfections and also Doppler shifts**. To take it into account, we assume a Brownian phase offset evolution [14]:

$$\theta_k = \theta_{k-1} + w_k \quad k \geq 2 \quad (4)$$

where w_k is an i.i.d. zero-mean Gaussian noise sequence with known variance $\frac{\sigma_w^2}{S}$ where σ_w^2 stands for the variance of the phase increment in one symbol interval. We note that the variance of the Gaussian noise is directly related to the rapidity of evolution of the phase. The $N \times N$ covariance matrix of the phase offset $\boldsymbol{\theta} = [\theta_1 \cdots \theta_N]^T$ is

$$\boldsymbol{\Sigma} = \frac{\sigma_w^2}{S} \begin{pmatrix} 1 & 1 & 1 & \cdots & 1 \\ 1 & 2 & 2 & \cdots & 2 \\ 1 & 2 & 3 & \cdots & 3 \\ \vdots & \vdots & \vdots & \ddots & \\ 1 & 2 & 3 & & N \end{pmatrix} + \sigma_{\theta_1}^2 \mathbf{1} \quad (5)$$

with an inverse that takes a tridiagonal form.

2.3. State-Space Model

When using an optimal filtering approach, a state-space model formulation is needed. Moreover, as we want to take into account that the observation noise on the output of the matched filter is not white, we must include it into the state evolution.

First of all we consider a sliding vector $[\nu_k \ \nu_{k-1} \ \cdots \ \nu_{k-S+1}]^T$ over an i.i.d. noise n_k , the evolution of this vector can be written as

$$\begin{bmatrix} \nu_k \\ \nu_{k-1} \\ \vdots \\ \nu_{k-S+1} \end{bmatrix} = \begin{bmatrix} 0 & \cdots & \cdots & 0 \\ 1 & 0 & \cdots & 0 \\ 0 & \ddots & & \vdots \\ & & & 1 & 0 \end{bmatrix} \begin{bmatrix} \nu_{k-1} \\ \nu_{k-2} \\ \vdots \\ \nu_{k-S} \end{bmatrix} + \begin{bmatrix} n_k \\ 0 \\ \vdots \\ 0 \end{bmatrix}$$

The coloured noise b_k is

$$b_k = [\Pi_0 \cdots \Pi_{S-1}] \begin{bmatrix} \nu_{k-1} \\ \nu_{k-2} \\ \vdots \\ \nu_{k-S} \end{bmatrix}$$

The state includes the phase offset and the coloured noise:

$$\mathbf{x}_k = [\theta_k \ b_k \ \nu_k \ \cdots \ \nu_{k-S+1}]^T$$

We define

$$\mathbf{M}_K = \begin{bmatrix} 1 & 0 & 0 & \cdots & & 0 \\ 0 & 0 & \Pi_0 & \Pi_1 & \cdots & \Pi_{S-1} \\ 0 & 0 & 0 & 0 & \cdots & 0 \\ \vdots & 0 & 1 & 0 & \cdots & 0 \\ & \vdots & 0 & 1 & & \vdots \\ & & & \ddots & \ddots & \ddots \\ & & & & 0 & 1 & 0 \end{bmatrix}$$

and $\mathbf{w}_k = [w_k \ 0 \ n_k \ 0 \ \cdots \ 0]^T$. From this, the state evolution is

$$\mathbf{x}_k = \mathbf{M}_K \mathbf{x}_{k-1} + \mathbf{w}_k \quad (6)$$

and the observation equation can be written as

$$\begin{aligned}
 y_k &= A_k \exp(i [1 \ 0 \ \cdots \ 0] \mathbf{x}_k) \\
 &+ [0 \ 1 \ 0 \ \cdots \ 0] \mathbf{x}_k \\
 &= A_k \exp(i\theta_k) + b_k
 \end{aligned} \tag{7}$$

We note that the state equation is linear whereas the observation equation depends non-linearly on the state. With this formulation, there is no observation noise because we have included it in the state.

3. Bayesian Cramér-Rao Bound

In estimation problems, we aim to know the ultimate accuracy that can be achieved by the estimator. Cramér-Rao Bounds (CRB) provide lower bounds on the Mean Square Error (MSE) achievable by any unbiased estimator. Depending on the nature of the parameters, several CR bounds exist. If the vector of parameters is deterministic, we use the standard CRB whereas, if the vector of parameters is random and an *a priori* information is available, we use the so-called Bayesian CRB [15]. When dealing with both random and deterministic parameters, an Hybrid CRB (HCRB) is used [16]. The CRB suited to our problem is the BCRB as we want to estimate the phase offset evolution vector $\boldsymbol{\theta}$ which is a random vector with an *a priori* probability density function (pdf) $p(\boldsymbol{\theta})$.

In the on-line synchronization mode, at time k the receiver updates the observation vector $\mathbf{y} = [y_1 \cdots y_{k-1}]^T$ including the new observation y_k to obtain the updated vector $\mathbf{y} = [y_1 \cdots y_k]^T$ in order to estimate θ_k : only the past and the current observations are available. In this section, we recall the expression of the Bayesian CRB and we present the closed-form expression of the BCRB for an oversampled phase offset estimation problem in a Data Aided scenario, which is a simpler closed-form expression of the bound than the one we presented in [12].

3.1. BCRB: background

We have a set of N measurements \mathbf{y} that depends on the N -dimensional vector of parameters to be estimated, $\boldsymbol{\theta}$. The joint probability density function of the pair $(\mathbf{y}, \boldsymbol{\theta})$ is $p_{\mathbf{y}, \boldsymbol{\theta}}(\mathbf{y}, \boldsymbol{\theta})$ and the *a priori* pdf is $p(\boldsymbol{\theta})$. If $\hat{\boldsymbol{\theta}}(\mathbf{y})$ is our estimate of $\boldsymbol{\theta}$, the BCRB satisfies the following inequality on the MSE:

$$E_{\mathbf{y},\boldsymbol{\theta}} \left\{ [\hat{\boldsymbol{\theta}}(\mathbf{y}) - \boldsymbol{\theta}][\hat{\boldsymbol{\theta}}(\mathbf{y}) - \boldsymbol{\theta}]^T \right\} \geq \mathbf{B}^{-1}$$

where \mathbf{B} is the so-called Bayesian Information Matrix (BIM) defined as [1]

$$\mathbf{B} = E_{\mathbf{y},\boldsymbol{\theta}} \left[-\Delta_{\boldsymbol{\theta}}^{\boldsymbol{\theta}} \log p(\mathbf{y}, \boldsymbol{\theta}) \right]$$

Expanding the log-likelihood, the BIM can be rewritten as

$$\mathbf{B} = \mathbf{B}^D + \mathbf{B}^P \tag{8}$$

with

$$\mathbf{B}^D = E_{\mathbf{y},\boldsymbol{\theta}} \left[-\Delta_{\boldsymbol{\theta}}^{\boldsymbol{\theta}} \log p(\mathbf{y} | \boldsymbol{\theta}) \right]$$

$$\mathbf{B}^P = E_{\boldsymbol{\theta}} \left[-\Delta_{\boldsymbol{\theta}}^{\boldsymbol{\theta}} \log p(\boldsymbol{\theta}) \right]$$

where the first term represents the average information about $\boldsymbol{\theta}$ brought by the observations \mathbf{y} and the second term represents the information available from the prior knowledge on $\boldsymbol{\theta}$, *i.e.*, $p(\boldsymbol{\theta})$.

The $N \times N$ BCRB matrix is

$$\mathbf{BCRB} = \mathbf{B}^{-1} = \{\mathbf{B}^D + \mathbf{B}^P\}^{-1} \tag{9}$$

where the k^{th} element of the diagonal, $[\mathbf{BCRB}]_{k,k}$, represents the lower bound on the estimation of $[\boldsymbol{\theta}]_k$ from observations $\mathbf{y} = [y_1 \cdots y_N]^T$.

3.2. BCRB: Application to Dynamical Phase Offset Estimation

In this paragraph, a closed-form expression for the BCRB for an on-line fractionally-spaced phase-offset estimation problem is presented.

We use the model presented in Section II (eqs.4,7):

$$\begin{aligned} \theta_k &= \theta_{k-1} + w_k \\ y_k &= A_k \exp(i\theta_k) + b_k \end{aligned}$$

where, as stated before, b_k is a non-white noise with covariance matrix $\boldsymbol{\Gamma}$. The index k refers to t_k instants and A_k are the coefficients specified in (eq.2).

To compute the BIM, the likelihood function and the *a priori* pdf are needed. From the model, the log-likelihood is

$$\log p(\mathbf{y} | \boldsymbol{\theta}) = \log \frac{1}{\pi^N |\det(\mathbf{R})|} - [\mathbf{y} - \mathbf{m}]^H \boldsymbol{\Gamma}^{-1} [\mathbf{y} - \mathbf{m}] \tag{10}$$

where \mathbf{y} is the N -dimensional received signal array and \mathbf{m} is the mean vector of \mathbf{y} , where the k^{th} component is $[\mathbf{m}]_k = A_k e^{i\theta_k}$. The logarithm of the *a priori* pdf is

$$\log p(\boldsymbol{\theta}) = \log p(\theta_1) + (N-1) \log \left(\frac{1}{\sqrt{2\pi}\sigma_w} \right) - \sum_{k=2}^N \frac{(\theta_k - \theta_{k-1})^2}{2\sigma_w^2} \quad (11)$$

The first term of eq.(8) can be computed from eq.(10). We note $\Lambda(\boldsymbol{\theta}) = \log p(\mathbf{y} | \boldsymbol{\theta})$. Computing the derivative with respect to the l^{th} and k^{th} elements of $\boldsymbol{\theta}$ we have that

$$\frac{\partial^2 \Lambda(\boldsymbol{\theta})}{\partial \theta_k \partial \theta_l} = 2\Re \left\{ \frac{\partial^2 \mathbf{m}^H}{\partial \theta_k \partial \theta_l} \boldsymbol{\Gamma}^{-1} [\mathbf{y} - \mathbf{m}] - \frac{\partial \mathbf{m}^H}{\partial \theta_l} \boldsymbol{\Gamma}^{-1} \frac{\partial \mathbf{m}}{\partial \theta_k} \right\}$$

The $(k, l)^{th}$ element of the matrix \mathbf{B}^D is

$$\begin{aligned} [\mathbf{B}^D]_{k,l} &= E_{\boldsymbol{\theta}} \left\{ E_{\mathbf{y}|\boldsymbol{\theta}} \left\{ -\frac{\partial^2 \Lambda(\boldsymbol{\theta})}{\partial \theta_k \partial \theta_l} \right\} \right\} \\ &= E_{\boldsymbol{\theta}} \left\{ 2\Re \left\{ \frac{\partial \mathbf{m}^H}{\partial \theta_l} \boldsymbol{\Gamma}^{-1} \frac{\partial \mathbf{m}}{\partial \theta_k} \right\} \right\} \\ &= 2\Re \left\{ A_l^* A_k \cdot [\boldsymbol{\Gamma}^{-1}]_{k,l} E_{\boldsymbol{\theta}} \left\{ e^{j(\theta_k - \theta_l)} \right\} \right\} \end{aligned}$$

We can write that

$$\begin{aligned} E_{\boldsymbol{\theta}} \left\{ e^{i(\theta_k - \theta_l)} \right\} &= E_{\boldsymbol{\theta}} \left\{ e^{i(\mathbf{u}_{kl}^T \boldsymbol{\theta})} \right\} \\ &= \phi(\mathbf{u}_{kl}) \end{aligned}$$

where $\mathbf{u}_{kl}^T = [0, \dots, 0, (+1), 0, \dots, 0, (-1), 0, \dots, 0]$, $+1$ in the k^{th} position and -1 in the l^{th} position of the array, $\phi(\cdot)$ is the characteristic function of a Gaussian random variable $\boldsymbol{\theta}$:

$$\begin{aligned} \phi(\mathbf{u}_{kl}) &= \exp \left\{ -\frac{1}{2} \mathbf{u}_{kl}^T \boldsymbol{\Sigma}^{-1} \mathbf{u}_{kl} \right\} \\ &= \exp \left\{ -\frac{1}{2} \left([\boldsymbol{\Sigma}^{-1}]_{k,k} + [\boldsymbol{\Sigma}^{-1}]_{l,l} - 2 [\boldsymbol{\Sigma}^{-1}]_{k,l} \right) \right\} \end{aligned}$$

with $\boldsymbol{\Sigma}$ the covariance matrix of the phase evolution $\boldsymbol{\theta}$ (eq.(5)). Finally

$$[\mathbf{B}^D]_{k,l} = 2\Re \left\{ A_l^* A_k [\boldsymbol{\Gamma}^{-1}]_{k,l} e^{\Psi_{k,l}} \right\}$$

where

$$\Psi_{k,l} = \left\{ -\frac{1}{2} \left([\boldsymbol{\Sigma}^{-1}]_{k,k} + [\boldsymbol{\Sigma}^{-1}]_{l,l} - 2 [\boldsymbol{\Sigma}^{-1}]_{k,l} \right) \right\}$$

We note that $[\Sigma^{-1}]$ takes a tridiagonal form, so the elements $[\Sigma^{-1}]_{k,l}$ are only non-null if $|k-l| \leq 1$. If we consider $\sigma_{\theta_1}^2 = 0$, they take the following values:

- $[\Sigma^{-1}]_{|k-l|=1} = -S/\sigma_w^2$
- $[\Sigma^{-1}]_{k,k} = 2\frac{S}{\sigma_w^2}$, for $2 < k < N-1$
- $[\Sigma^{-1}]_{1,1} = [\Sigma^{-1}]_{N,N} = S/\sigma_w^2$

So we have to consider two cases:

- $\Psi_{k,k} = 0$ for $k = l$
- $\Psi_{k,l} = -\beta\frac{S}{\sigma_w^2}$ for $|k-l| \geq 1$

with $1 \leq \beta \leq 3$ if $\sigma_{\theta_1}^2 = 0$

We can finally conclude that $e^{\Psi_{k,l}} \sim 0$ for small values of σ_w^2 when $k \neq l$. The worst case is when $\sigma_{\theta_1}^2 = 0$, $k = 1$, $l = N$ and $S = 1$; in this case, we have $\Psi_{1,N} = -\frac{1}{\sigma_w^2}$, and so $e^{\Psi_{k,l}} = e^{-\frac{1}{\sigma_w^2}}$ can be neglected for $\sigma_w^2 \leq 0.1$ compared to the main diagonal elements.

As we assume the phase variation is small over the symbol interval (for the approximation in eq.(1) to be valid), we can consider that \mathbf{B}^D is a diagonal matrix with

$$[\mathbf{B}^D]_{k,k} = 2 |A_k|^2 [\mathbf{\Gamma}^{-1}]_{k,k} \quad (12)$$

In the sequel, we compute the second term of eq.(8). From the state evolution eq.(4) we have that

$$\Delta_{\boldsymbol{\theta}} \ln p(\boldsymbol{\theta}) = \Delta_{\boldsymbol{\theta}} \ln p(\theta_1) + \sum_{k=1}^N \Delta_{\boldsymbol{\theta}} \ln p(\theta_k | \theta_{k-1}) \quad (13)$$

The first term in eq.(13) is a matrix with only one non-zero element, namely, the entry (1, 1), which is equal to

$$\left[\Delta_{\boldsymbol{\theta}} \ln p(\theta_1) \right]_{1,1} = \frac{\partial^2 \ln p(\theta_1)}{\partial \theta_1^2}$$

The other terms are matrices with only four non-zero elements, namely, the entries $(k-1, k-1)$, $(k-1, k)$, $(k, k-1)$ and (k, k) . Due to the Gaussian nature of the noise, one finds

$$\begin{aligned} \left[\Delta_{\boldsymbol{\theta}} \ln p(\theta_k | \theta_{k-1}) \right]_{k,k} &= \left[\Delta_{\boldsymbol{\theta}} \ln p(\theta_k | \theta_{k-1}) \right]_{k-1,k-1} \\ &= \frac{-S}{\sigma_w^2} \end{aligned}$$

$$\begin{aligned} \left[\Delta_{\boldsymbol{\theta}} \ln p(\theta_k | \theta_{k-1}) \right]_{k,k-1} &= \left[\Delta_{\boldsymbol{\theta}} \ln p(\theta_k | \theta_{k-1}) \right]_{k-1,k} \\ &= \frac{S}{\sigma_w^2} \end{aligned}$$

Assuming that $E_{\theta_1} \left[\Delta_{\boldsymbol{\theta}} \ln p(\theta_1) \right] = 0$ (non-informative prior about θ_1 , see [2]), we obtain that

$$\mathbf{B}^P = \frac{1}{\sigma_w^2/S} \begin{pmatrix} 1 & -1 & 0 & \cdots & 0 \\ -1 & 2 & -1 & \ddots & \vdots \\ 0 & \ddots & \ddots & \ddots & 0 \\ \vdots & & -1 & 2 & -1 \\ 0 & \cdots & 0 & -1 & 1 \end{pmatrix} \quad (14)$$

From eqs.(12,14) we have that the BIM has a tridiagonal form

$$\mathbf{B} = \beta \begin{pmatrix} (C_1 + 1) & 1 & & & \\ & 1 & C_2 & 1 & \\ & & \ddots & \ddots & \ddots \\ & & & 1 & C_{N-1} & 1 \\ & & & & 1 & (C_N + 1) \end{pmatrix}$$

with $\beta = -S/\sigma_w^2$ and $C_k = (1/\beta) [\mathbf{B}^D]_{k,k} - 2$.

The on-line bound for the estimation of θ_N is equal to entry (N, N) of the inverse of the BIM, $[\mathbf{B}^{-1}]_{N,N}$. From [26] we have that the elements of the diagonal of the inverse of a tridiagonal matrix are

$$[\mathbf{B}^{-1}]_{k,k} = \frac{d_{k-1}h_{k+1}}{d_k}$$

with

$$\begin{aligned} d_k &= \beta C_k d_{k-1} - \beta^2 d_{k-2} \quad \text{for } k = 2, \dots, N-1 \\ h_k &= \beta C_k h_{k+1} - \beta^2 h_{k+2} \quad \text{for } k = 2, \dots, N-1 \end{aligned} \quad (15)$$

and

$$\begin{aligned}
d_0 &= 1, d_1 = \beta (C_1 + 1) \\
d_N &= \beta (C_N + 1) d_{N-1} - \beta^2 d_{N-2} \\
h_1 &= \beta (C_1 + 1) h_2 - \beta^2 h_3 \\
h_N &= \beta (C_N + 1), h_{N+1} = 1
\end{aligned}$$

Finally, the on-line BCRB is

$$BCRB = [\mathbf{B}^{-1}]_{N,N} = \frac{d_{N-1}}{d_N} \quad (16)$$

We note that this is directly the cofactor of the element $[\mathbf{B}]_{N,N}$ over the determinant of \mathbf{B} .

3.2.1. Remarks

As we analyse the estimation problem in a DA scenario the bound depends on the transmitted sequence \mathbf{a} . In this paper, we suppose the transmission of a known sequence to analyse the performance of the proposed algorithm and the bound. We note that, contrary to [12] where the proposed bound was the minimum over a set of sequences, the BCRB is now computed for a specific transmitted sequence.

However, for $S = 1$, $s = 0$ (symbol reference point) and $\tau = 0$, eq.(12) shows that the bound is independent of the transmitted sequence \mathbf{a} since $|A_k| = 1 \forall k$. In other cases, the bound depends on the sequence, the over-sampling factor S and the position s inside the current transmitted symbol (index M):

$$BCRB(\mathbf{a}, S, s) = [\mathbf{B}^{-1}(\mathbf{a})]_{N,N} \quad (17)$$

with $N = (M - 1) * S + 1 + s$.

3.2.2. User's manual

Here we give a short user's manual for the derivation of the Bayesian CRB for the phase estimation problem. As symbols are known and since we suppose that we know the statistics of the observation and phase noises, we can easily obtain the bound by two different ways: computing the matrix $[\mathbf{B}]$ and then his inverse, or computing the elements C_k and recursively compute the bound.

1. Direct derivation of the BCRB:

- Compute the matrix $[\mathbf{B}^D]$ from eq.(12).

- Compute the matrix $[\mathbf{B}^P]$ from eq.(14).
 - Compute the inverse of the BIM (eq.(9)) and take the last element to have the on-line BCRB (eq.(17)).
2. Alternative derivation using recursion formulas:
- Compute the coefficients C_k , from the elements $[\mathbf{B}^D]_{k,k}$ (eq.(12)).
 - Use the recursion formula eq.(15) to obtain eq.(16).

4. Extended Kalman Filter

In the sequel, we derive the EKF [7] for oversampled carrier phase estimation. The system is described by the following state-space equations pair

$$\begin{aligned}\mathbf{x}_{k+1} &= f_k(\mathbf{x}_k) + \mathbf{w}_k \\ \mathbf{y}_k &= g_k(\mathbf{x}_k) + \mathbf{v}_k\end{aligned}$$

where \mathbf{x}_k is the state vector, \mathbf{w}_k is a zero-mean white noise with covariance matrix \mathbf{Q}_k , \mathbf{y}_k is the observation vector at time k which is a partial and noisy observation of the state \mathbf{x}_k and \mathbf{v}_k is the observation noise with covariance matrix \mathbf{R}_k . Noises \mathbf{w}_k and \mathbf{v}_k are supposed to be uncorrelated. The functions $f_k(\cdot)$ and $g_k(\cdot)$ can be non-linear in a general case.

We note $\hat{\mathbf{x}}_{k|m}$, the estimation of \mathbf{x}_k from observations up to time m , $\tilde{\mathbf{x}}_{k|m} = \mathbf{x}_k - \hat{\mathbf{x}}_{k|m}$, the estimation error and $\mathbf{P}_{k|m} = \text{E}(\tilde{\mathbf{x}}_{k|m}\tilde{\mathbf{x}}_{k|m}^T)$ its covariance matrix.

For Gaussian, linear state models, the KF gives the best Mean Square Error (MSE) estimation of the state \mathbf{x}_k from observations up to time k .

For non linear problems, the EKF gives a sub-optimal estimator $\hat{\mathbf{x}}_{k|k}$ in a recursive way: the main idea is to linearize the state-space equations at each iteration in order to transform the filtering problem into a usual Kalman one.

4.1. EKF for Dynamical Phase-Offset Estimation

To derive the EKF, we need to compute $\partial f_k(\mathbf{x}_k)/\partial \mathbf{x}_k$ and $\partial g_k(\mathbf{x}_k)/\partial \mathbf{x}_k$. In the state-space model for oversampled phase estimation presented in Section II (eqs.(6,7)), the state equation is linear, hence $\partial f_k(\mathbf{x}_k)/\partial \mathbf{x}_k = \mathbf{M}_K$. The state noise covariance \mathbf{Q} is independent from k and has only two non-zero elements : $[\mathbf{Q}]_{1,1} = \sigma_w^2/S$ and $[\mathbf{Q}]_{3,3} = \sigma_n^2$. Because we introduced the

coloured noise b_k into the state, there is no observation noise and the covariance matrix \mathbf{R} is null. Since the observation equation is non-linear versus the state, we have to apply a linearization:

$$\mathbf{g} = \frac{\partial g_k(\hat{\mathbf{x}}_{k|k-1})}{\partial \mathbf{x}_k} = \begin{bmatrix} iA_k e^{i\hat{\theta}_{k|k-1}} & 0 & 1 & 0 & \dots & 0 \end{bmatrix}^T \quad (18)$$

Finally, the EKF-based algorithm is:

$$\left\{ \begin{array}{l} \mathbf{P}_{k|k-1} = \mathbf{M}_K \mathbf{P}_{k-1|k-1} \mathbf{M}_K^H + \mathbf{Q} \\ \hat{\mathbf{x}}_{k|k-1} = \mathbf{M}_K \hat{\mathbf{x}}_{k-1|k-1} \\ \mathbf{K}_k = \mathbf{P}_{k|k-1} \mathbf{g}^H \{ \mathbf{g} \mathbf{P}_{k|k-1} \mathbf{g}^H \}^{-1} \\ \mathbf{P}_{k|k} = [\mathbf{I} - \mathbf{K}_k \mathbf{g}] \mathbf{P}_{k|k-1} \\ \hat{\mathbf{x}}_{k|k} = \hat{\mathbf{x}}_{k|k-1} + \mathbf{K}_k \left[\mathbf{y}_k - A_k e^{i\hat{\theta}_{k|k-1}} - \hat{b}_{k|k-1} \right] \end{array} \right.$$

where \mathbf{I} is the identity matrix with appropriate dimension. We note $\hat{\mathbf{x}}_{0|0}$ and $\mathbf{P}_{0|0}$, the initial state and covariance matrix, which are set to an arbitrary value in the range of convenience (*i.e.*, for the phase offset we take as initial value an uniformly distributed random number in $[0, 2\pi)$).

We explicit the dependence of the EKF MSE on S and s with the notation $\text{MSE}_{\text{EKF}}(S, s)$ for the MSE of an EKF working on the s^{th} point of each symbol of a S -time oversampled signal.

5. Discussion

In this section we show the behaviour of the BCRB and the EKF by considering different scenarios. We also compare the results obtained with well-known bayesian estimation methods (Particle Filter and Unscented Kalman Filter) to justify the use of the EKF, and we analyse the performance loss when using a real world shaping function . We assume the transmission over an AWGN channel of a M-sequence of length 511 bits, generated using a Linear Feedback Shift Register (LFSR) with characteristic polynomial $[1021]_8$ (octal representation). We consider three oversampling factors ($S = 1, 2$ and 4) and a BOC shaping pulse (see figure 2). BOC shaping pulse is used in Galileo positioning system [4].

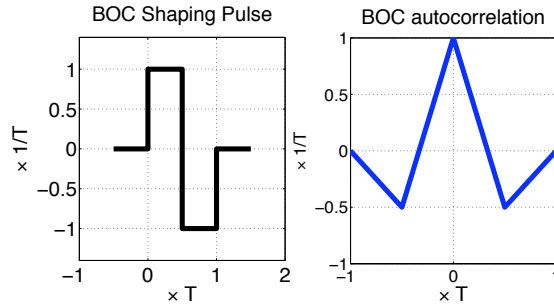


Figure 2: BOC shaping function $\Pi(t)$ and its autocorrelation $g(t)$

In the figures, we plot the MSE obtained by Monte Carlo simulations versus the Signal to Noise Ratio (SNR). The SNR corresponds to the Carrier to Noise Ratio ($\frac{C}{N}$) at the input of the receiver. In our case, as shaping pulse and symbols a_k are normalised (*i.e.* $\sigma_a^2 = 1; g(0) = 1$) this ratio is simply $\frac{C}{N} = \frac{1}{\sigma_n^2}$. For the MSE we consider two cases:

1. We compute $BCRB(\mathbf{a}, S, 0)$ and $MSE_{EKF}(S, 0)$ for the T -spaced symbol reference point estimation for $S = 1, 2, 4$.
2. We compute the MSE for the mid-point estimation ($s = S/2$). This scenario is also interesting because the intermediate points can be useful when using fractionally-spaced algorithms (*i.e.* half symbol spaced equalizer or Gardner's timing recovery algorithm).

5.1. T -spaced symbol reference point estimation MSE

Figures 3 and 4 superimpose, versus the SNR, the on-line BCRB (see eq.(16)) and the EKF MSE. For figure 3, we have a slow varying phase with variance $\sigma_w^2 = 0.001 \text{ rad}^2$ and for figure 4, a phase with a faster evolution, $\sigma_w^2 = 0.01 \text{ rad}^2$. In both scenarios there is no offset from the optimal sampling instants, $\tau = 0$.

For $S = 1$, the performance of the EKF fits the BCRB. For $S = 2$, the EKF performance is slightly looser than the bound. For $S = 4$, EKF MSE is only slightly better than for $S = 2$ at high SNR; furthermore, the EKF no longer fits the bound.

The gain increases with the oversampling factor S and the interest of oversampling becomes clear at low SNR. The gain due to oversampling decreases as the SNR increases.

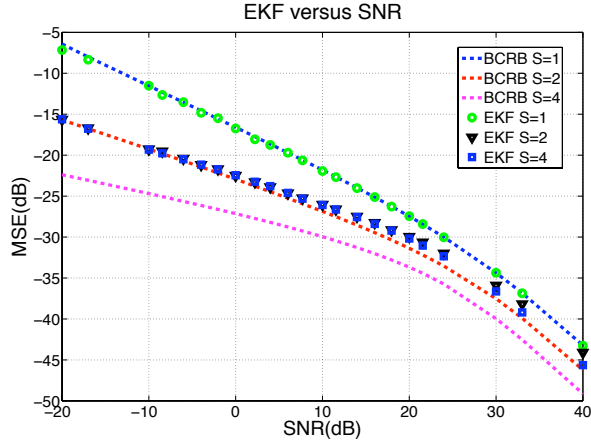


Figure 3: EKF MSE and BCRB versus the SNR for three different oversampling factors $S = 1, 2$ and 4 , with a phase-noise variance $\sigma_w^2 = 0.001 \text{ rad}^2$.

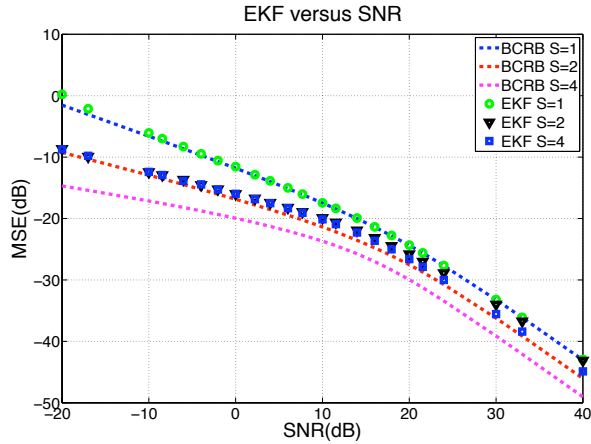


Figure 4: EKF MSE and BCRB versus the SNR for three different oversampling factors $S = 1, 2$ and 4 , with a phase-noise variance $\sigma_w^2 = 0.01 \text{ rad}^2$.

In figure 5, we analyse the EKF behaviour for a fixed SNR versus phase-noise variance for a low SNR value (0 dB). Here, we can still measure the gain given by the oversampling and the good performance of the algorithm. The gain obtained with the oversampling is greater at weak σ_w^2 . We also note that the performance of the algorithm at weak phase noise variance is really close to the bound. At very high σ_w^2 the performances become poorer compared to the bound. This is probably because, for high σ_w^2 , the modeling

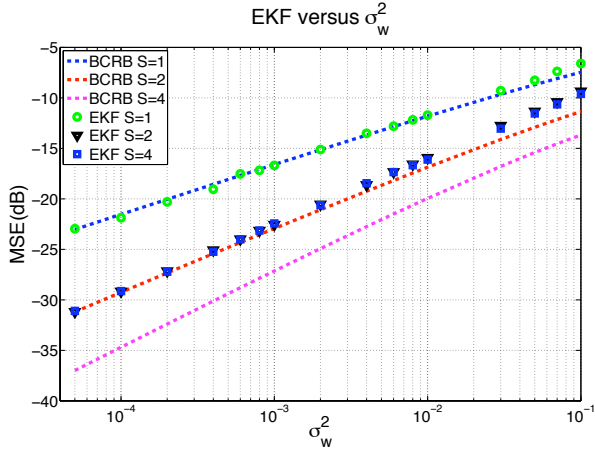


Figure 5: EKF MSE and BCRB versus the phase noise variance for three different oversampling factors $S = 1, 2$ and 4 , $\text{SNR} = 0\text{dB}$.

error in the EKF linear approximation (see eq.(18)) is not negligible with respect to the noise level.

Figure 6 superimposes versus the SNR, the on-line BCRB, $BCRB(S, 0)$, and the EKF for a slow varying phase evolution, $\sigma_w^2 = 0.001$, and a non-null offset $\tau = \frac{T}{8}$ for $S = 1, 2$. As a reference, we plot the performance of the EKF for a null offset $\tau = 0$. For $\tau \neq 0$, the bound and the algorithm are looser. The gain between different oversampling factors is greater at high SNR when having a non-null offset.

To show that performances decrease when τ increases, we plot in figure 7, the on-line BCRB and the EKF versus τ . We consider $0 \leq \tau < \frac{T}{4}$, a fixed $\text{SNR}=0\text{dB}$ and a slow varying phase evolution, $\sigma_w^2 = 0.001$. We note that the performance for $S = 4$ is symmetric with τ each $\frac{T}{8}$, for $S = 2$ each $\frac{T}{4}$ and for $S = 1$ each $\frac{T}{2}$.

5.2. T -spaced symbol mid-points estimation MSE

We now take the $S = 4$ case as the reference. For $S = 1$, there is only 1 estimate per symbol, so, to compare with $S = 2, 4$, missing mid-points are generated by blocking the estimated value ($s = 0$) over the symbol period. We will note it $\text{MSE}_{\text{EKF}}(1, 1/2)$

The BCRB for the blocked case $S = 1$ can be easily obtained as

$$BCRB_b(\mathbf{a}, 1, 1/2) = BCRB(\mathbf{a}, 1, 0) + \sigma_w^2/2.$$

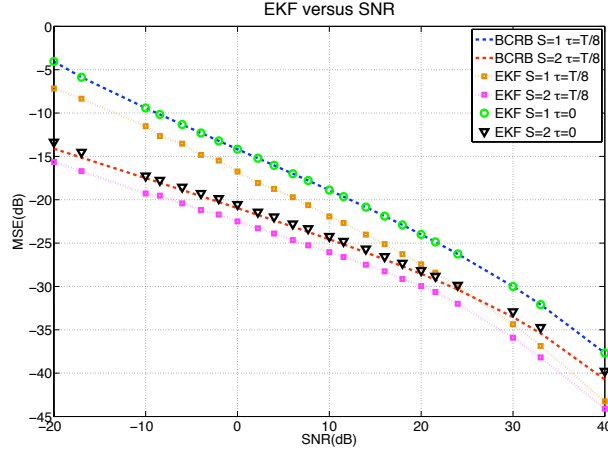


Figure 6: EKF MSE and BCRB versus the SNR in presence of a non null offset for the sampling instants for two different oversampling factors $S = 1$ and 2 .

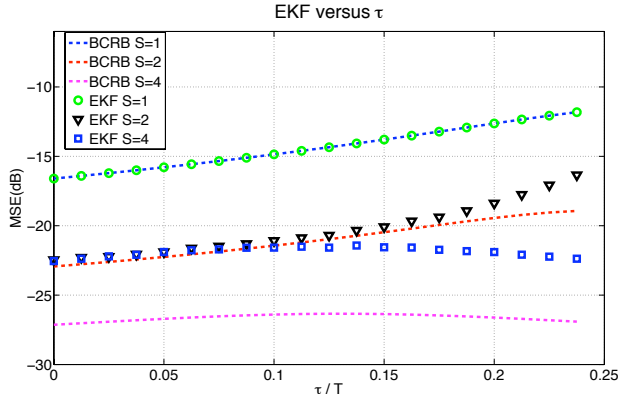


Figure 7: EKF MSE and BCRB versus τ for $\text{SNR}=0\text{dB}$ and $\sigma_w^2 = 0.001$.

For $S > 1$, the bound strongly depends on the last observed value A_N because of the non-stationary power. In this case, we rename the bound as $BCRB(A_N, S, s)$. For $\tau = 0$, $|A_N|$ can be equal to 0 or 1 (see fig.1), so there are two possible bounds. We can define an average bound as follows:

$$BCRB(S, s) = p_0 \cdot BCRB(|A_N|=0, S, s) + (1 - p_0) \cdot BCRB(|A_N|=1, S, s) \quad (19)$$

where p_0 is the proportion of $A_k = 0$. This average bound is completely

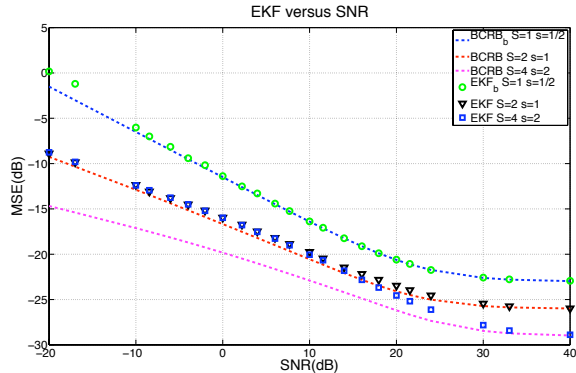


Figure 8: EKF and BCRB versus the SNR for the mid points, three different oversampling factors $S = 1, 2$ and 4 , and a phase-noise variance $\sigma_w^2 = 0.01 \text{ rad}^2$.

suites to compare with the MSE performance of the EKF computed with the same proportion p_0 . In our simulation $p_0 = 0.5$.

5.2.1. Results

For the mid-points case, figure 8 superimposes, versus the SNR, the on-line BCRBs ($BCRB_b(1, 1/2)$, $BCRB(2, 1)$, $BCRB(4, 2)$) and the EKF MSE for a fast varying phase with variance $\sigma_w^2 = 0.01 \text{ rad}^2$ and a null offset $\tau = 0$. For $S = 1$ and 2 , the variance of the EKF is close to the BCRB. For $S = 4$, at low SNR, the MSE of the EKF is almost the same than for $S = 2$ and tends to the bound at high SNR.

The gain increases with the oversampling factor S , the interest of oversampling becomes clear at low SNR. At high SNR, $MSE \rightarrow \sigma_w^2/2S$, this is due to the blocking process for $S = 1$ and to the non-stationary power sequence A_k for $S = 2$ and 4 . We can also see this saturation from eq.(19) which for $p_0 = 0.5$ at high SNR becomes

$$BCRB(S, s) \sim \frac{1}{2}BCRB(0, S, s)$$

and so $BCRB(0, S, s) = \sigma_w^2/S$. If we compare the performance of the algorithm in this case with the performance at $s = 0$ (see fig.4) we can see that we obtain the same result at low SNR and looser performance at high SNR because of the saturation.

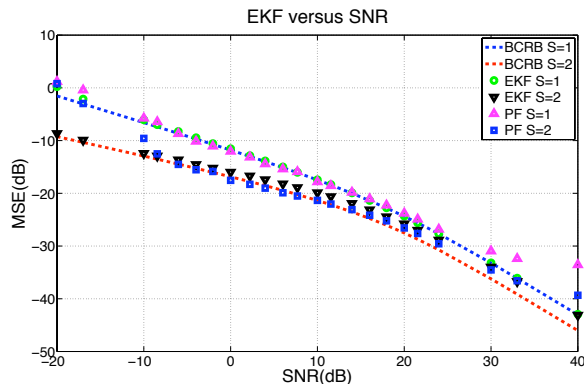


Figure 9: EKF, PF and BCRB versus the SNR for two different oversampling factors $S = 1, 2$, with a phase-noise variance $\sigma_w^2 = 0.01 \text{ rad}^2$.

5.3. Comparison with Bayesian methods and real world analysis

The goal of this paragraph is twofold. First, we want to compare the performance of the EKF with a Bayesian method, a Sequential Importance Sampling with Resampling Particle Filter (PF) which uses a residual resampling algorithm. This method represent the most important family of Bayesian estimators: Sequential Monte Carlo methods [9, 10, 11].

Secondly, we show the performances obtained with the EKF when using a limited bandwidth real world shaping pulse. In this case we take a band limited BOC function, which is a BOC function convoluted with a *sinc* function. So the shaping function is no longer rectangular.

Both analysis are done on the T-spaced symbol reference point case. The parameters not specified, are the same that we stated at the beginning of the section. In the second case, the signal is bandlimited but the algorithm is the same as for the ideal BOC function.

5.3.1. Comparison

Figures 9 superimposes, versus the SNR, the on-line BCRB and the MSE obtained with two different algorithms: the EKF and the PF. We use 50 particles in the PF. We have a moderate varying phase with variance $\sigma_w^2 = 0.01 \text{ rad}^2$ and $\tau = 0$.

For $S = 1$, the results obtained with the PF are the same that using the EKF, except for high SNR, where the PF performance is looser. For $S = 2$, the performance of the PF is slightly better between 5dB and 25dB, but looser at really low and high SNR.

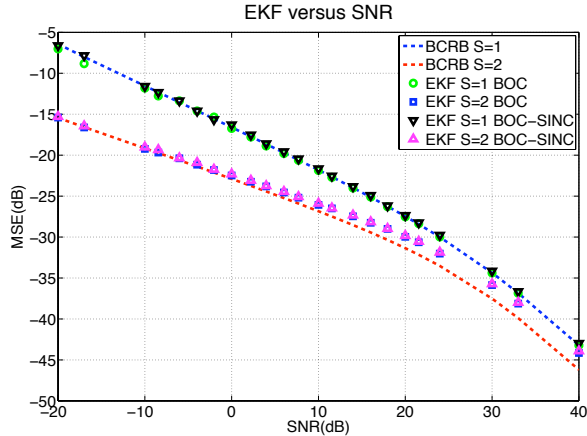


Figure 10: EKF MSE for two BOC shaping functions and BCRB versus the SNR for two different oversampling factors $S = 1, 2$, with a phase-noise variance $\sigma_w^2 = 0.001 \text{ rad}^2$. $W = 4/T$.

The complexity and computational load of the PF is much higher than the EKF, which is the simplest nonlinear filtering method. The PF is difficult to tune, and the fact that we have to evaluate the functions for each particle, makes it computationally really expensive. Moreover, the results are mostly the same or a bit looser. For these reasons, in this kind of problems, only slightly nonlinear and with low state dimension, the EKF is still the best option.

5.3.2. Real world analysis

We present in figure 10, the comparison between the results obtained with the BOC shaping function from fig.2 and using a real life limited bandwidth BOC shaping function.

This limited bandwidth BOC is obtained by filtering the ideal BOC shaping function with a $\text{sinc}(\pi Wt)$. We note that for Galileo, we have a chip rate $1/T = 10 \text{ Mchip/sec}$, and the frequency carrier receiver bandwidth is $W = 20 \text{ MHz}$ (*i.e* $2/T$) or $W = 40 \text{ MHz}$ (*i.e* $4/T$), which allows us to take advantage of an oversampling of, respectively, $S = 2$ and $S = 4$, samples/symbol, which is usual in satellite receivers.

We present the results obtained with a phase noise variance $\sigma_w^2 = 0.001 \text{ rad}^2$, $\tau = 0$ and a bandwidth $W = 4/T$.

The results using the limited bandwidth BOC shaping does not change

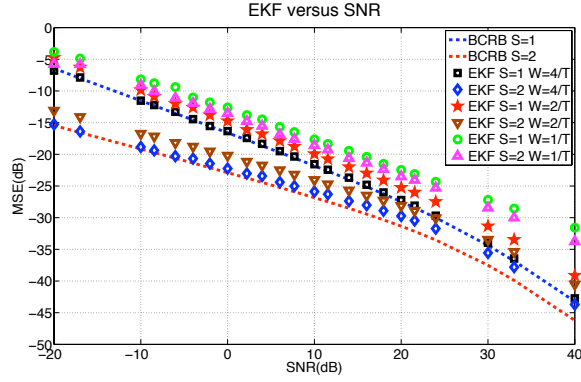


Figure 11: EKF MSE for a limited bandwidth BOC shaping function ($W = 1/T, 2/T$ and $4/T$) versus the SNR, for two different oversampling factors $S = 1, 2$, with a phase-noise variance $\sigma_w^2 = 0.001 \text{ rad}^2$.

from the results obtained with the ideal BOC function. The receiver's bandwidth is large enough when computing the performance with the EKF for $S = 1, 2$ and 4.

In figure 11, we present the results obtained in the same scenario, but using a *sinc* function with three different bandwidths, $W = 4/T, 2/T$ and $1/T$. We can see that in the first case, $W = 4/T$ the results are the same as using the ideal BOC function. Using $W = 2/T$ and $W = 1/T$, it is clear that the bandwidth is not large enough and the performance are much looser (loss of 2.5dB for $W = 2/T$ and up to 8dB for $W = 1/T$ and $S = 2$). As it is usual in satellite receivers to have $S = 4$ samples/symbol, we can conclude that the results obtained with the ideal BOC shaping function are valid in the real world scenario.

We note that, if slow-rate data bits superimpose the training sequence, the algorithm does not work correctly when the modulating value is -1 . We can easily overcome this problem by starting in parallel the algorithm for both values, $+1$ and -1 , and rapidly detecting the proper value, for example, from the Kalman filter estimation covariance. Then we only go on running the algorithm with the decided value .

6. Conclusion

In usual transmission systems, the roll-off is between 0 and 100%; hence, one or two samples per symbol are enough to recover the whole information

about the analog received signal. However, in the context of satellite positioning systems, like GPS and GALILEO, time limited shaping pulse are used and the Nyquist-Shannon sampling theorem does not apply. These special conditions let us hope a significant receiver synchronization performance improvement when the received signal is oversampled.

In this paper, we study the gain due to an oversampling of the received signal for the problem of dynamical carrier phase tracking. Assuming the data are known at the receiver, we derive the Bayesian Cramér-Rao Bound and a Kalman-based DA algorithm for carrier phase estimation in such an oversampled scenario.

This study shows several improvements when a fractionally-spaced method for phase estimation is used. The estimation MSE decreases as the oversampling factor S increases, the interest of oversampling is more important at low SNR.

For $S = 1$ or 2 samples per symbol, the results obtained with the EKF are close to the theoretical bound for slow and moderate phase evolutions. For $S = 4$, the BCRB is lower than for $S = 2$ but the EKF performance does not show the same improvement.

When using a limited bandwidth BOC or the ideal BOC shaping function, we obtain the same performance in standard satellite communications scenarios if the bandwidth is large enough. But we have also seen the limitations of the algorithm when having an extremely rapidly varying phase evolution with respect to the symbol interval.

We have shown that the use of most sophisticated techniques, (*i.e.* Bayesian filters), computationally heavier and more difficult to tune, are not necessary in this case. We obtain mostly the same performances, or slightly looser, than using the EKF.

Acknowledgement

This work was supported in part by the French ANR (Agence Nationale de la Recherche), LURGA project.

References

- [1] H. L. Van Trees, *Detection, Estimation and Modulation Theory*. New York: Wiley, 1968, vol.1.

- [2] S. M. Kay, *Fundamentals of statistical signal processing: estimation theory*. Upper Saddle River, NJ, USA: Prentice Hall, Inc., 1993.
- [3] U. Mengali and A.N. D'Andrea, *Synchronization Techniques for Digital Receivers*. Plenum Press, NY, USA, 1997.
- [4] European Space Agency / Galileo Joint Undertaking. *Galileo Open Service Signal in Space Interface Control Document - Draft 1*. 2008.
- [5] R. E. Kalman, "A new approach to linear filtering and prediction problems", *J. Basic Eng., Trans. ASME*, Series D, vol. 82, No.1, pp. 35-45, 1960.
- [6] R. E. Kalman and R. S. Bucy "New results in linear filtering and prediction theory", *J. Basic Eng., Trans. ASME*, Series D, vol. 83, No.3, pp. 95-108, 1961.
- [7] B. D. O Anderson and J. B. Moore, *Optimal Filtering*. Englewood Cliffs, NJ, USA: Prentice Hall, 1979.
- [8] A. H. Jazwinski, *Stochastic Processes and Filtering Theory*. Academic Press, Inc. , NY, 1970.
- [9] A. Doucet, N. de Freitas, and N. J. G. Eds., *Sequential Monte Carlo Methods in Practice*. New York, N.Y.: Springer-Verlag, 2001.
- [10] A. Doucet, S. J. Godsill, and C. Andrieu, "On sequential Monte Carlo sampling methods for Bayesian filtering", *Statistics and computing*, vol. 10, pp. 197-208, 2000.
- [11] S. Arulampalam, S. Maskell, N. Gordon, T. Clapp, "A Tutorial on Particle Filters for On- line Non-linear/Non-Gaussian Bayesian Tracking", *IEEE Trans. on Signal Processing*, vol. 50, pp. 174-188, 2002.
- [12] J.Vilà Valls, J. M. Brossier and L. Ros, "On-line Bayesian Cramér-Rao bound for oversampled dynamical phase offset estimation", *IEEE ISCCSP 2008*, Malta, 12-14 March 2008.
- [13] J.Vilà Valls, J. M. Brossier and L. Ros, "Extended Kalman Filter for oversampled dynamical phase offset estimation", *IEEE ICC 2009*, Dresden, Germany, 14-18 June 2009.

- [14] P. O. Amblard, J. M. Brossier and E. Moisan, “Phase tracking: what do we gain from optimality? Particle filtering versus phase-locked loops”, *Elsevier Signal Processing*, vol. 83, pp. 151-167, Oct. 2003.
- [15] S. Bay, C. Herzet, J. M. Brossier, J. P. Barbot, and B. Geller, “Analytic and Asymptotic Analysis of Bayesian Cramér-Rao Bound for Dynamical Phase Offset Estimation”, *IEEE Trans. Signal Processing*, vol. 56, pp. 61-70, Jan. 2008.
- [16] S. Bay, B. Geller, A. Renaux, J. P. Barbot, and J. M. Brossier, “On the Hybrid Cramér Rao Bound and Its Application to Dynamical Phase Estimation”, *IEEE Signal Processing Letters*, vol. 15, pp. 453-456, 2008.
- [17] P. Tichavský, C. H. Muravchik, A. Nehorai, “Posterior Cramér-Rao bounds for discrete-time nonlinear filtering”, *IEEE Trans. Signal Processing*, vol. 46, pp. 1386-1396, May 1998.
- [18] A. N. D’Andrea, U. Mengali and R. Reggiannini, “The modified Cramér-Rao bounds and its applications to synchronization problems”, *IEEE Trans. Commun.*, vol. 42, pp. 1391-1399, Feb.-Apr. 1994.
- [19] F. Gini, R. Reggiannini and U. Mengali, “The modified Cramér-Rao bound in vector parameter estimation”, *IEEE Trans. Commun.*, vol. 46, pp. 52-60, Jan. 1998.
- [20] B. M. F. Rice, B. Cowley and M. Rice, “Cramér-Rao Lower Bounds for QAM Phase and Frequency Estimation”, *IEEE Trans. Commun.*, vol. 49, pp. 1582-1591, Sept. 2001
- [21] W. G. Cowley, “Phase and frequency estimation for PSK packets: bounds and algorithms”, *IEEE Trans. Commun.*, vol. 44, pp. 26-28, Jan. 1996
- [22] P. J. Kootsookos, “An extended kalman filter for demodulation of polynomial phase signals”, *IEEE Signal Processing Letters*, Vol. 5, No. 3, March 1998.
- [23] B. F. La Scala, R. R. Bitmead “Design of an extended kalman filter frequency tracker”, *IEEE Signal Processing Letters*, Vol. 5, No. 3, March 1998.

- [24] A. Aghamohammadi, H. Meyr, G. Ascheid“ Adaptive synchronization and channel parameter estimation using an extended kalman filter”, *IEEE Trans. on Communications*, Vol. 37, No. 11, Nov. 1989.
- [25] L.-L. Cheng, Z.-G. Cao “GPS Carrier phase measurement method based on data transition detection in high dynamic circumstance”, *Proc. WCC-ICCT*, Vol.2, 21-25 Aug. 2000.
- [26] R. Usmani, “Inversion of Jacobi’s tridiagonal matrix”, *Computers Math. Applic.*, vol. 27,no. 8 pp. 56-59, 1994.